10 Molecular dynamics simulations, the theoretical partner to static SIMS experiments

Barbara J. Garrison
Department of Chemistry, Penn State University, University Park, PA 16802, USA.
E-mail: bjg@psu.edu

10.1 Introduction

Secondary ion mass spectrometry (SIMS) is a wonderful technique for providing mass spectrometric information of molecules on surfaces as demonstrated in other articles in this volume. For example, positive and negative SIMS spectra of an alkanethiol overlayer adsorbed on a metal substrate shown in Figure 1 exhibit numerous identifiable peaks.[1a] The parent thiolate mass (M) is discernable from peaks in the negative spectrum, although metal ions are attached. There is a characteristic pattern of pairs of peaks at $C_nH_{2n-1}^+$ and $C_nH_{2n+1}^+$, which indicates an alkane chain. In addition, there are peaks such as AuS^- and $Au(CH_2)_2^+$ that do not readily provide useful information.

Naturally, we would like to understand the fundamental events that give rise to the spectrum shown in Figure 1, especially if such an understanding would help interpret spectra. In addition, a fundamental understanding allows one to think about possible new applications as well as limitations of the technique. So, what is the conceptual understanding of phenomena in a SIMS experiment?

One often hears the phrase that the primary ion establishes a collision cascade in the solid. To me a collision cascade implies a sophisticated pool game as shown in Figure 2 for an Ar atom striking a film of alkanethiolate molecules adsorbed on a Au surface.[2] From this animation and many more animations with different initial position of Ar hits, a visual picture of the process begins to emerge. In this case, the primary Ar particle strikes the organic film, first creating organic fragments. These species then damage the film while the Ar particle hits the metal substrate. Further action within the metal substrate creates an uplifting motion that induces the lift-off of entire parent molecules.[5] The visualisation in Figure 2 has been generated from classical molecular dynamics (MD) computer simulations.

The focus of this chapter is to discuss the MD approach and to present exemplary results from the simulations. Before embarking on the discussion, a preview of how the MD simulations can be used to interpret the mass spectrum of alkanethiols is presented. As discussed below, there are some approximations and limitations in the MD approach. Two points are of note here. First, the classical approximation assumes that there is only

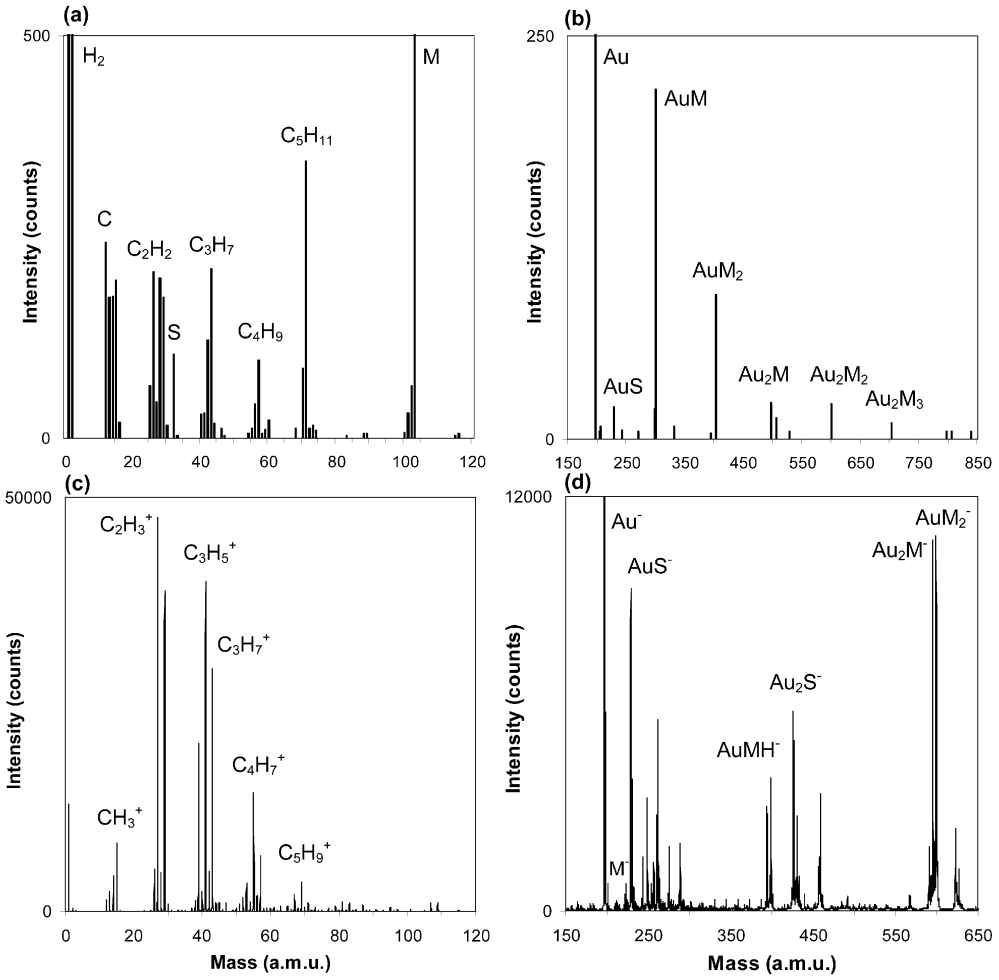

Figure 1. Calculated and experimental mass spectra of alkanethiolates on Au. (a,b) Calculated spectra of neutral species at 1 ps after the Ar impact. Reprinted with permission from Reference 2. Copyright 1999 American Chemical Society. (c) Experimental positive ion spectrum in low mass regime. Reprinted with permission from Reference 1. Copyright 1998 Surface Spectra. (d) Experimental negative ion spectrum in high mass regime Reprinted with permission from Reference 1. Copyright 1998 Surface Spectra.

one electronic state for the system, thus no ionisation effects are explicitly included. The MD results must therefore be critically assessed before making direct comparisons to experimental SIMS data. Second, because the classical equations of motion are being integrated numerically with a small time step, only a few picoseconds (ps) of real time are followed. Events that might occur during the microsecond (μs) flight time to the experimental detector must be inferred.

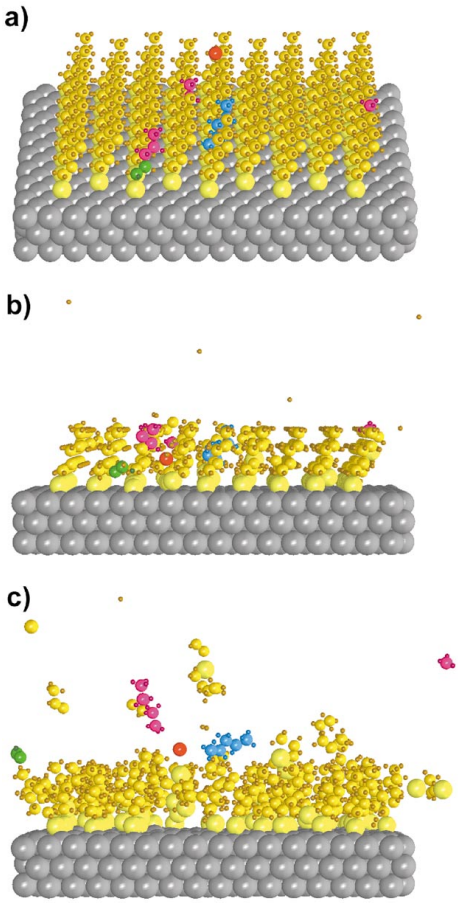

Figure 2. Positions of atoms as a function of time for a MD simulation of Ar (red sphere) bombardment of an alkanethiolate (yellow spheres) overlayer adsorbed on Au (grey spheres). (a) 0 fs, (b) 100 fs, (c) 500 fs. The large, medium and small yellow spheres represent S, C and H atoms. Pink spheres denote fragments that have been clipped from the tops of chains, green spheres denote an ejected acetylene molecule and the blue spheres a C_5H_{12} formed by reaction between two molecules. Six additional layers of Au atoms were used in the simulation.

Given the stated above caveats (neutral species, ~1 ps after the bombardment event), the calculated mass spectrum for an alkanethiol layer on Au is shown in Figure 1. The animations judiciously scrutinised by a human make the following predictions. Many of these predictions are not specific to the thiolate system and have been observed for other systems of upright chains on surfaces.

- The C_nH_{2n+1} fragments predominantly arise from clipping of the tops of the chains during the collision cascade as shown in Figure 2. The clipped fragments are shown in pink.

- Since the C_nH_{2n-1} species do not appear in the simulations, it is inferred that they arise due to unimolecular decay of $C_nH_{2n+1}^+ \rightarrow C_nH_{2n-1}^+ + H_2$ during the μs flight to the experimental detector.
- The simulations predict as much C_nH_{2n} and C_nH_n as well as C_nH_{2n+1}. Although these alkene and alkyne species are not observed in SIMS spectra, they are observed in experiments in which neutral ejected species are postionised.[1b] An ejected acetylene molecule is shown in green in Figure 2.
- The small species such as H, C, S, CH, CH_2 and C_2H readily form during the collision cascade and are observed in experimental spectra. The simulations also predict the formation of H_2 molecules and that ~80% of these molecules form from H atoms from two different molecules.[3] There are individual H and C atoms apparent in frames (b) and (c) of Figure 1.
- Gold–thiolate (Au_xM_y) clusters are observed in both the calculations and experimental spectra. Specific predictions are made from the simulations with respect to the original local bonding geometry of the partners in the complexes.[2] For example, we find that 99% of the thiolate molecules in the AuM_2 clusters originated from nearest neighbour sites on the surface.

In contrast to the successful comparison delineated above, there are also some areas of disagreement. The simulations do not predict the appearance of SH, $Au(CH_2)$ and $Au(CH_2)_2$. Some of these missing peaks are understandable in terms of the inadequacy of the interaction potential, an input to the simulations. Some of the differences are not, as yet, understandable.

Overall, I feel the successes of the MD simulation approach are sufficiently good that they provide a useful aid to experimentalists. *Any point of disagreement between measured and calculated results provides us the opportunity to improve the model and perhaps even perform a reality check for the experimental results*.

This article first discusses the MD approach in a manner that I hope establishes a firm conceptual basis of the technique for experimental SIMS practitioners. Full descriptions and details of the MD approach are given elsewhere. After a description of the technique, I will show how the MD approach has been used to describe the static SIMS process and interpret experimental data. The emphasis is placed on simulations of molecular systems rather than atomic solids. After discussing the successes of the MD approach, we point out the areas where future efforts are desirable.

There are two complementary chapters in this volume. Herbert Urbassek has written a chapter on collision cascade theory.[4] Collision cascade theory attempts to describe analytically the essential features of the bombardment process and works quite well for many processes in atomic solids. Arnaud Delcorte's chapter describes the fundamental processes in organic SIMS from an experimental viewpoint.[5] He intertwines results from MD simulations into his chapter in order to elucidate the microscopic events underlying experimental measurements.

Finally, the word sputter is used in this chapter as shorthand for the physics of ejecting particles from the surface due to energetic particle bombardment. This definition is the conventional one used by others.

10.2 Description of MD simulations

The emphasis in this section is on describing the essential elements of molecular dynamics (MD) simulations along with possible ramifications on what can be calculated. Recipes for actually performing simulations are published elsewhere.[6–12] The essential items covered here include the inherent assumptions of classical mechanics, the force or interaction potential, numerical integration and time step choice, initial and final conditions and their relationship to experimental conditions, asking the right questions of the simulations and finally, how to get started doing simulations.

From Sir Isaac Newton over 300 years ago we have the following second-order differential equation that governs the motion of classical particles:

$$m_i \times \mathbf{a}_i = m_i \times \mathrm{d}^2\mathbf{r}_i/\mathrm{d}t^2 = \mathbf{F}_i = - \quad V(\mathbf{r}_1, \mathbf{r}_2, \ldots \mathbf{r}_{N\,\mathrm{atoms}}) \tag{1}$$

or as recast into first-order differential equations by Sir William Rowan Hamilton

$$m_i \times \mathrm{d}\mathbf{v}_i/\mathrm{d}t = \mathbf{F}_i \tag{2a}$$

$$\mathrm{d}\mathbf{r}_i/\mathrm{d}t = \mathbf{v}_i \tag{2b}$$

where m_i, $\mathbf{r}_i$, $\mathbf{v}_i$, $\mathbf{a}_i$ and $\mathbf{F}_i$ are the mass, position, velocity, acceleration and force of the i^{th} particle. The particles discussed here are atoms and there are a total of N_{atoms} of them in the system. The interaction potential, $V(\mathbf{r}_1, \mathbf{r}_2, \ldots \mathbf{r}_{N\,\mathrm{atoms}})$, is generally a function of the positions of all the atoms. The position, velocity, acceleration and force are all vectors in three dimensions. Quite simply the pictures in Figure 2 were obtained by numerically integrating the equations of motion (Equation 2) for $N_{\mathrm{atoms}} \approx 4000$ particles with an appropriate interaction potential.

Molecular dynamics simulations are not unique to sputtering and have been used to describe a plethora of phenomena including atom–diatom scattering, structure of liquids, diamond film growth, motion of galaxies and sand dunes and protein folding. Interestingly, one of the first applications of MD simulations being performed on a computer was sputtering of a Cu target by Gibson, Goland, Milgram and Vineyard in 1960.[13] Shortly after this study, the late Don E. Harrison Jr initiated his pioneering work on computer simulations of sputtering.[14] Many of the ideas and concepts that we currently reinvent were first identified by Harrison in his simulations of sputtering of Cu solids.

10.2.1 Assumptions of classical mechanics

The equations of motion of Newton are, in fact, classical in nature. No quantum effects of any kind are included and no excited electronic or ionic states are taken into account. Thus, ionisation is beyond the scope of classical mechanics. As discussed below,

we generally assume that the particles are in their lowest electronic state during all the motions. There is no coupling or transfer of energy between the electronic and nuclear degrees of freedom.

Several workers have tried to develop methods for incorporating specific quantum mechanical effects into the MD model. Frictional forces to account for energy losses to the electronic modes have been used.[6] A curve-crossing model[15] to account for energy losses in the first few hard collisions[16,17] as well as to predict the energy distributions of Rh atoms ejected in the $^4F_{7/2}$ excited fine structure state[18] has been successfully applied. The classic work of Yu and Lang predicts ion intensities as a function of workfunction.[19] In all these examples, the simulations helped determine the ramifications of a specific quantum model on the dynamics but the simulations did not *predict* the quantum mechanical effect that was important. At this stage, full predictive quantum calculations are beyond our theoretical and computational ability.

The omission of quantum effects including excited electronic states and ions does limit some of the questions we can hope to address with the simulations. On the other hand, *the nuclear motion of the atoms (and molecules) underlies all other processes*. Understanding how the particles move is the first step in understanding everything else. If we invoke some other physics or chemistry to explain data without understanding the contribution from the nuclear motion, then we are probably deceiving ourselves as to our real knowledge of the process.

10.2.2 Force or interaction potential

The essential ingredient in either Equation 1 or Equation 2 for describing realistically atomic motions, especially in the chemical regime, is the nature of the force or interaction potential. In undergraduate physical chemistry terms, the interaction potential is the solution to the electronic Schrödinger equation within the Born–Oppenheimer approximation.[20] In principle, one could solve the Schrödinger equation for each configuration of atoms shown in Figure 2 and evaluate the forces. Computer speeds are not sufficient, however, to even begin to consider a direct evaluation of the Schrödinger equation during the simulations with thousands of particles.[21] Thus, the approach most commonly employed is to use a mathematical equation with a functional form that can represent the actual solution of the Schrödinger equation. The parameters of the functional form are then fit to available experimental data, preferably from experiments other than SIMS experiments.[22]

A simple empirical potential energy curve vs separation distance for a diatomic molecule is shown in Figure 3. There are three basic regions. First, at large internuclear separation, the potential (and force) must be zero, as the atoms do not know about the presence of one another. At distances appropriate for bonding (equilibrium bond length), the potential energy should be the dissociation energy. The curvature near the minimum in the potential energy is related to the vibrational frequency of the molecule. At internuclear separations smaller than that shown in Figure 3, the nuclear–nuclear repulsion interaction dominates and the potential becomes highly repulsive.

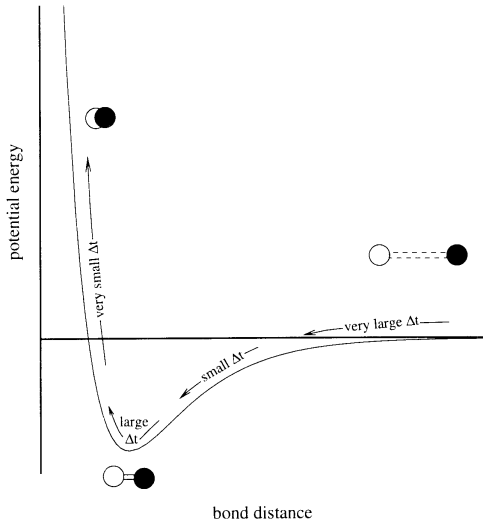

Figure 3. Morse potential vs distance.

All regions of the interaction potential are important. The repulsive wall dominates the interactions during the first few hard collisions when one of the particles has hundreds to tens of thousands of electron volts of kinetic energy. The repulsive wall gives a measure of the size of the particles and is an important factor in modelling the openness of the system to the incoming particle. As the energy of the system becomes dispersed among the atoms, however, the lower energy part of the wall is important until finally the bonding region dominates. The dissociation energy (or cohesive energy in a solid) directly influences how easy it is to separate the atoms or remove a particle from the solid in the case of sputtering. In addition, the low-energy part must reflect any chemistry in the system.

Developing a potential for a diatomic molecule is relatively straightforward as generally there are data for the equilibrium bond strength, bond length and vibrational frequency, as well as some information about the size (repulsive wall) at high collision energies. The challenge comes when there are many atoms. The simplest potential for an atomic solid such as Cu is a pairwise additive or pair potential. The assumption is that each pair of atoms interacts via a potential similar to that shown in Figure 3 and that this interaction is independent of the presence of other atoms.[23] Pair potentials have served the sputtering community quite well over the years especially for atomic solids. After all, much of the dynamics in the system is dictated by the placement of atoms. If an incoming particle sees an atom directly in its way, then a collision will occur. If the incoming particle sees a channel, then it will pass through the solid.

Pair potentials become inadequate when one wants to examine processes that involve the bonding region or chemistry of the system and for systems that are not close-packed arrays of atoms. The pairwise additive assumption predicts that a triatomic molecule will have an equilibrium geometry of an equilateral triangle and that the total attrac-

tive interaction is three times that of the diatomic molecule. Certainly, ozone, O_3, does not have an equilateral triangle geometry and is not three times more stable than O_2. Triatomic H_3 is not even a stable molecule. There are even problems describing solid Cu. For example, if one fits the dissociation energy in the pair potential to the bulk cohesive energy, then the value of the dissociation energy is ~0.5 eV. The dissociation energy of diatomic Cu_2, however, is ~2 eV. Thus, if one is interested in the ejection of diatomic molecules, the calculations with pair potentials cannot simultaneously give the right energy for atoms in the bulk and in a diatomic molecule.

During the 1980s, efforts were made by several groups to develop empirical potentials for reactions that include many-body effects, that is, the interaction between a pair of atoms changes depending on other atoms nearby.[24] The most developed potentials are those for face centred cubic metals and group IV (silicon, germanium and carbon) elements. Examples of popular potentials for face centred cubic (fcc) metals include the Sandia embedded atom method (EAM)[25] and the molecular dynamics-Monte Carlo corrected effective medium MD/MC-CEM[26,27] potentials. For Si, popular potentials have been developed by Stillinger–Weber[28] and Tersoff.[29] One potential of recent interest to the SIMS community was developed by Brenner for reactions of hydrocarbon molecules.[30] The bond strength changes depending on the coordination number, bond angles and conjugation effects, and therefore, the potential is able to model bond breaking and bond formation. Brenner conceived a sufficiently flexible functional form that he could fit it to the plethora of experimental data available for bulk phases of carbon as well as small molecules. His initial interest was modelling diamond film growth but other researchers have used the potential for a variety of processes in which reactions can and do occur.[31]

The capability of the Brenner potential to describe hydrocarbon reactions is exemplified in Figure 4. The system under investigation is the sputtering of an overlayer of ethylidyne (–C–CH_3) on a Pt surface due to bombardment by Ar. At 15 fs into the collision cascade, each C atom has a tetrahedral bonding geometry with four neighbouring atoms. By 50 fs, one ethylidyne molecule has been ejected by a collision with a substrate atom and one H atom has migrated to the other C atom forming $HCCH_2$. This species continues to move above the surface with excess internal energy. At sometime between 95 and 125 fs, the excited $HCCH_2$ spits out a H atom to form a stable acetylene, HCCH, molecule. The bonding geometry around the acetylene molecule is linear as is appropriate. The Brenner potential describes smoothly the change in bonding geometry and energy of an atom as the number of neighbours changes. This potential is by no means perfect. There is no long range van der Waals type interaction included, thus one cannot predict the density of ethylidyne molecules on the Pt surface. As an aside, several potentials exist that do model the density of organic and biological molecules quite well.[32–35] These potentials for biological simulations, however, cannot describe bond breaking and reforming reactions. Finally, Stuart, Harrison and Tutein have incorporated a long-range interaction term to the Brenner potential in a manner so that the interactions between non-bonded species can occur.[36] We look forward to trying the new AIREBO potential for simulations of molecular solids.

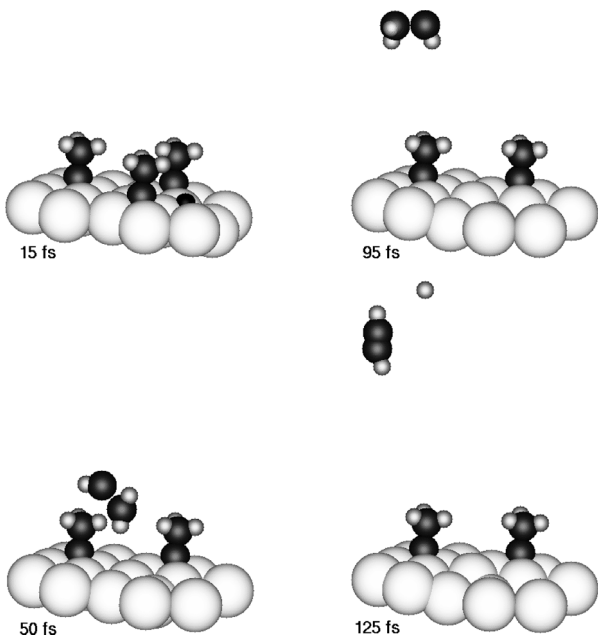

Figure 4. Unimolecular rearrangement and fragmentation of C_2H_3 yielding HCCH. Reprinted with permission from Reference 65. Copyright 1995 American Chemical Society.

Regardless of the interaction potential that is used in the simulations, the model system of particles has all the physics of a real system including cohesive energy, equilibrium geometry, vibrational frequencies, compressibility, speed of sound, surface tension etc. The model system can undergo phase transitions. *Thus, even if the properties of the model system do not perfectly match those of a real system, it is possible to use the model system to develop general ideas of the various processes that might occur.* It is important, though, to know what properties of the model system are comparable to the real system and not to over interpret results from the simulations. More discussion on asking the right questions of the simulation is given below.

10.2.3 Numerical integration and time step

Solving the equations of motion, Equation 2, involves numerical integration. For two reasons, Hamilton's equations are generally solved rather than Newton's equation. First, ultimately we want both the positions and velocities of all the particles as a function of time and Newton's equations would only give the positions. Second, algorithms for solving first-order differential equations are more developed than for solving second-order equations. The challenge to solving Equation 2 is that the force, **F**, is a function of all the positions. The positions depend on the time. The standard approach in numerical integration is to assume that **F** is approximately constant over a small time interval or time step, δt. Then one can write the solution to Equation 2 as

$$\mathbf{v}_i(t + \delta t) = \mathbf{v}_i(t) + \mathbf{F}_i[\mathbf{r}(t)]/m_i \times \delta t \tag{3a}$$

$$\mathbf{r}_i(t + \delta t) = \mathbf{r}_i(t) + \mathbf{v}_i(t) \times \delta t \tag{3b}$$

where δt is chosen such that $\mathbf{F}(t)/m$ and $\mathbf{v}(t)$ are nearly constant during the time step.[37] The evolution of all the positions and velocities during the collision cascade thus occurs in discrete steps. As discussed in the next section, knowledge of the velocities allows one to calculate quantities such as angles of motion, kinetic energy, temperature and pressure. The positions as a function of time yield a microscopic picture of the motions as shown in Figures 2 and 4. The positions and velocities combined together give information about molecules and clusters.

The algorithms for solving Equation 3 with a good integration scheme are well developed and can be found in a number of articles on sputtering or MD simulations. Briefly, though, the catch in solving Equation 3 is the condition that δt be chosen such that $\mathbf{F}(t)/m$ and $\mathbf{v}(t)$ are nearly constant during the time step. From Figure 3 we see that $\mathbf{F}(t) = -\nabla\, V(\mathbf{r})$ is nearly constant when the particles are far apart and when the particles are near their equilibrium separation. On the other hand, $\mathbf{F}(t)$ changes most quickly at small internuclear separations when two particles are undergoing a near head-on collision. So for particles a long distance apart or near equilibrium, a large time step can be used. For head-on collisions a small time step must be used. In addition to the force, the mass of the particle influences the time step. Larger time steps can be used for heavier particles than for lighter particles. Hydrogen is particularly problematic because it is so light and moves so fast, that a very small time step must be taken. In almost all our simulations involving H, we assume the deuterated or tritiated form of H in order to take larger time steps. Chemically, the isotope of H makes no difference. There might be, however, small differences in reaction rates.

The criterion for an acceptable time step is whether energy is conserved as a function of time during the course of the numerical integration. This computational check is a very convenient aid in choosing the time step. Given that energy must be conserved, what is considered a large and small time step? We typically run our simulations with an integrator that allows us to vary automatically the time step during the collision cascade. Otherwise, we would have to use the smallest time step necessary for the first few head-on collisions for integration over the entire duration of the trajectory. Given in Table 1 are the ranges of time steps we have used for some sample systems. Times are given in 10^{-15} s or femtoseconds (fs).

Some trends are clear. The hydrocarbon system even with complete deuteration or tritiation requires the smallest time steps. Using a larger initial kinetic energy makes the smallest time step even smaller. Larger masses (Ag) allow larger time steps when the system is approaching the end of the cascade. Practically speaking, all of the values of the timesteps given in Table 1 are small. Due to algorithmic instabilities and computer round-off errors, only 10^6 to 10^8 integration steps can be made before spurious results start to appear in the solutions. Inherently MD simulations are limited to total times on the order of nanoseconds (ns). Fortunately, in many cases the sputtering process is over in 0.5–5 ps.

Table 1. Exemplary timesteps for different systems.

System	Energy of primary Ar particle	Range of time steps in fs
Alkanethiols on Au	700 eV	0.01–0.15
Silicon	1 keV	0.05–0.50
Ag	5 keV	0.03–10

10.2.4 Initial conditions

To initiate the integration of the equations of motion, Equation 3, the positions and velocities at time $t = 0$ must be prescribed for both the incoming particle as well as the substrate atoms. First, we will examine the initial conditions of the incident particle and then the substrate atoms.

10.2.4.1 Incoming particle

The choice of incoming particle can be made, in most cases, the same as in the experimental situation. The reason for the almost complete flexibility (in contrast to a limited choice of substrate) is that the primary particle imparts energy and momentum to the crystal and does not participate in the chemistry. Thus reasonable, purely repulsive interaction potentials can be constructed from Molière interaction forms.[38,39]

The initial velocity vector is chosen from the experimental energy and angle of incidence. Fortunately, most SIMS experiments are performed with monoenergetic beams and one does not have to worry about a thermal distribution of incident energies or angles. The initial position of the incident particle is chosen so that there is no interaction with the surface. In principle, the initial position would be at an infinite height from the surface. Almost all the potentials used in the MD simulations, however, go to zero at some separation as shown in Figure 3 so that "infinity" is somewhere between 5 and 20 Å. Finally, the incident particle must be aimed at a lateral position on the surface. Since the dynamics of the collision cascade are very different if the incident particle makes a head-on collision with one atom or enters a channel, one must calculate the motion in the solid for many different aiming points that represent all possible positions on the surface. For ordered systems such as shown in Figure 5, choosing the aiming area is straightforward. For disorder systems, care must be taken to sample representative areas of the surface. In the language of people who perform MD simulations, each aiming point of the primary particle and subsequent motion is called a trajectory.

The only new twist that has appeared recently is the use of polyatomic particles as incident particles. In these cases, one must choose many different angular orientations of the incident particle.[40] Fortunately, other scientific groups have developed prescriptions for proper averaging and one can actually even specify the initial vibrational and rotational quantum state[41] if the analogous experiment is of interest.

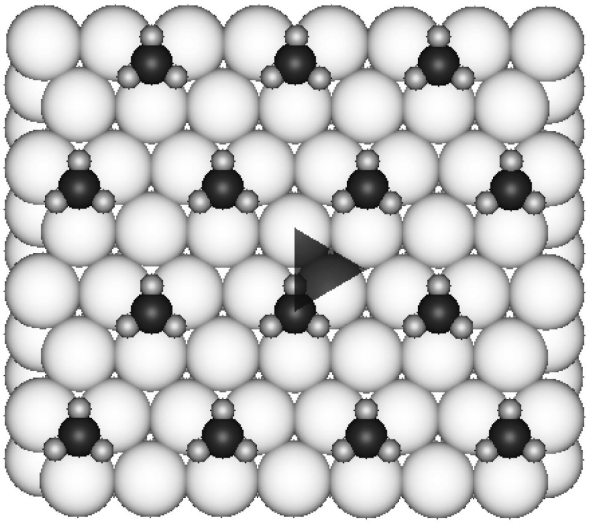

Figure 5. Triangular area for aiming incident particles for a quarter monolayer coverage of ethylidyne on Pt{111}. The Pt, C and H atoms are represented by the large, medium and small spheres, respectively. Reprinted with permission from Reference 65. Copyright 1995 American Chemical Society.

10.2.4.2 Substrate system

Innumerable times I have been asked the following question by experimentalists. "Can you model the system and events for my experiment?" Lately the answer has been "yes, if there is a reasonable interaction potential". That is, we have many of the necessary computational tools for modelling experiments except the interaction potential. A reasonable potential does not have to be a perfect potential. For example, the angular distributions of all fcc metals are very similar. Thus, a good potential for any fcc material will give insight into most experimental data. Certainly, we have used Si potentials to interpret data from experiments measuring angular distributions from GaAs surfaces.[42] Likewise, we used an interaction potential for Cu_3Au to model experimental data on Ni_3Al.[43] Unfortunately, there is a deficiency of good potentials for sputtering simulations of any organic/biological molecule that contains elements other than C or H; doped Si; GaAs, SiO_2; $NaBF_4$; etc.

The initial positions of the particles in the system are chosen to match best the experimental ones. For ordered systems (single crystals, ordered overlayers), the assignment of positions is relatively straightforward. If one, however, wants to model a disordered system, there are challenges. For example, if the experimental sample is a polycrystalline metal, can one really define the distribution of crystalline surfaces, the orientation of the crystallites at the surface, the size of the individual crystallites etc.? There is no magic answer here. One needs to use judgment and experience to figure out if a model system can be used to give insight into the experimental data.

The initial frame of Figure 2 and Figure 5 shows the initial placement of atoms for overlayers on single crystal metal surfaces. A finite number of particles have been used. In general, the number of atoms should be sufficiently large to contain all the important collisional events. One tries to be sensible in choosing the number of atoms. The more atoms in the system the more computer time is required for each aiming point of the primary particle on the crystal. The common practice is to run several aiming points on different crystal sizes and look for major changes in results. In general, the more motion that can be induced in the substrate, the bigger the crystal must be. Motion in the system tends to increase as the primary particle energy increases, if polyatomic primary particles are used or the binding energy of the species in the system is reduced.

Both the initial positions and velocities of the particles in the substrate should probably be chosen from a Maxwell–Boltzmann distribution. To make sure the motions are properly correlated, however, is a lot of work.[44] Except for a few special cases, the experimental data do not show any temperature dependence[45] so in general all initial velocities are zero and the particles start at their equilibrium positions.

As a final, somewhat technical note, we use open boundary conditions in the simulation. We allow particles that go out the sides or bottom of the crystal to leave the simulation. Physically, we assume that these energetic particles go deeper into the sample and do not create motion that gives to particles being ejected from the surface.

10.2.5 Final conditions

The numerical integration for one aiming point of the primary particle is terminated when no more particles can eject from the surface. Operationally, this condition occurs when the most energetic particle in the solid has less than some threshold value of energy. Once the trajectory is finished, one then examines pictorially or mathematically the final positions and velocities. The average yield of particles ejected can be determined by counting the particles above the surface and dividing by the number of aiming points calculated for the incident particles. The kinetic energy of the particles is $\frac{1}{2}m_i\mathbf{v}_i^2$. Calculating an energy distribution is a straightforward process. Likewise, the velocity vectors can be used to determine an angular distribution.

The final positions and velocities can be used to determine whether clusters and molecules ejected. More on this topic is discussed later as there are some subtleties associated with the question of whether the cluster will remain stable until it reaches the experimental detector several μs after the ejection event.

There are a number of properties that can be calculated for which there are no direct experimental measurements. For example, the calculations give the original position on the surface of the particles that eject relative to the initial impact point of the primary particle. The time that a particle ejects and the distribution of the number of particles ejected per incident particle can be monitored. The simulations also allow us to follow reaction mechanisms and see, for example, that much of the H_2 formed during sputtering of organic molecules arises from H atoms of different molecules.

Finally, the atomic motions giving rise to any particular event or sets of events can be extracted to understand *why* a certain event occurs. *It is the correlation of the microscopic basis of atomic motions with experimental data that, in my opinion, is the real strength of the MD simulations as a partner to static SIMS experiments.*

10.2.6 Changing one parameter at a time

A useful feature of the simulations is the ability to change one parameter at a time. For example, several years ago we were examining the sputtering of systems of alkane chains on diamond and Pt surfaces.[46] We found some striking differences and did not know whether the mass of the substrate, the openness of the diamond vs Pt surface or the interaction potentials were mainly responsible for the differences. In the simulations, it is trivial to change the mass of any element, for example C to a mass of 195 and Pt to a mass of 12 and rerun the simulations using the same interaction potentials and the same crystal structures. Thus, the effect of substrate mass on the collision dynamics could be investigated isolated from changes in structure and energetics. Similar adjustments can be made for many other parameters, for example, binding energy of an atom to the surface. These artificial systems yield insight as to the important factors in results.

10.2.7 Computer time

The total computer time depends on several factors including time step in the integration, total length of the motion from each aiming point of the primary particle, the number of trajectories that need to be sampled and the length of the force calculation. As given in Table 1, the range of time steps is 0.01 fs to ~1 fs. The total length of time of a trajectory can vary from a hundred fs to several ps if one is interested in large molecules[47] or large clusters[48] ejecting. The number of trajectories needed varies depending on the final quantities being calculated. For quantities such as total yield of particles emitted, perhaps 10–500 different aiming points are sufficient. On the other hand, for high-resolution energy and angle-resolved distributions often 3000–6000 aiming points are required.

The evaluation of the force is *the* most time-consuming part of each integration step. The computer time of the force calculation depends on several factors including the number of particles, the range of the force and the complexity of the force. For pair potentials, the force between each pair of atoms must be evaluated, thus there are approximately $N_{\text{atoms}}{}^2$ calculations. If the potential and force become zero at some distance as shown in Figure 3, then the number of evaluations can be reduced to $N_{\text{neighbours}} \times N_{\text{atoms}}$, where $N_{\text{neighbours}}$ is the number of neighbouring atoms with non-zero forces. By simple arguments, the number of neighbours of an atom scales as the cube of the distance at which the force becomes zero. In Table 2 are typical values for the number of neighbours with different potentials.

The complexity of the potential definitely influences the computer time. All many-body potentials are computationally more intensive than pair potentials. The AIREBO potential of Stuart *et al.* for long-range van der Waals CH interactions is even more complex than the many-body potentials for Si or Ag. In Table 3 are some current computer

Table 2. Typical number of neighbours for various interaction potentials.

Atom	Potential	Typical number of neighbours
H	Brenner CH	1
C	Brenner CH	4
Si	Stillinger–Weber or Tersoff	4
Ag	Sandia EAM or MD-MC/CEM	80
C or H	AIREBO	300

Table 3. Typical computer times for one trajectory on different systems.

System	N_{atoms}	$N_{molecules}$	Volume (1000 Å^3)	Incident energy (eV)	Time of trajectory	Computer time
Ag	3042		42	1000	1 ps	4 min
Alkanethiols on Au	3748	68 thiols 2592 Au	54	700	1 ps	50 min
Solid benzene	5760	480	56	100	1 ps	700 min

times for one trajectory along with the system size used and the kinetic energy of the incident particle. Metals and Si typically have cohesive energies of 4–6 eV so the system sizes in Table 3 are appropriate for ~1 keV Ar bombardment. The solid benzene system has a very small cohesive energy, and therefore, the primary particle must have less than 100 eV for a model system of comparable size. The alkanethiol calculation used only the Brenner potential whereas the solid benzene calculation used the long-ranged AIREBO potential.

The computational time issue is obvious. The computer times can be long per trajectory and many times thousands of trajectories are required. Examining high-energy particle bombardment of solid benzene will be a major computational effort.

10.2.8 MD and the BCA

Although not really part of this article, it is possible to mention the binary collision approximation (BCA) at this point in the discussion. The BCA is the approach used in several popular computer programs including TRIM[49] and MARLOWE.[50] It is discussed in more depth in the chapter by Urbassek[4] and a book by Smith *et al.*[12] In the BCA, it is assumed that only two particles collide and interact at a time whereas in MD simulations, all particles can simultaneously interact. The BCA only uses the repulsive wall of the

interaction potential. No attractive interactions or chemical reactions are part of the potential. Quantities used in BCA codes such as cohesive energy or surface binding energy are parameters. In other words, one cannot incorporate potentials such as the Brenner CH or MD/MC-CEM to model the sputtering of dimers or molecules.

The algorithm for evaluating dynamics using the BCA is different from the numerical integration of MD and is much faster. The BCA works well for examining implantation depths and ranges of high-energy particles. The dominant collisions are in the high-energy range and by using the BCA, large targets can be used. MD simulations of implantation would be impossible because the number of atoms required is computationally intractable. The strength of MD lies in its ability to use chemically meaningful potentials such that molecules, both organic and clusters of metal atoms, can be reasonably described.

10.2.9 Asking the right question

The main challenge in all of science including MD simulations is to understand which quantities or properties can be reliably calculated. It is easy to get "numbers" for many quantities from the simulations, but the values may be physically and chemically meaningless. Based on experience, below are some of my personal thoughts about what quantities can be addressed with MD simulations and which cannot.

- *Ions*. Predicting ion fractions is a tough, tough challenge without a good quantum mechanical model. All answers given below are predicated on the assumption that no quantum effects dominate.
- *Yields*. Average numbers of particles ejected are the easiest to calculate statistically. The absolute value of the yield, however, is heavily dependent on interaction potentials used in the simulation and of course the nasty issue of ionisation. It is best if one can examine relative yields as a function of ejection energy and angle, projectile energy or projectile mass.
- *Energy and angular distributions of ejected atoms*. The energy and angular distributions have been calculated quite reliably[11,51] over the years for two reasons. First, they represent relative yields. Second, they depend strongly on the placement of atoms in the substrate. Although, there is an effect of the interaction potential, it does not dominate the shape of the distributions.
- *Atomic vs polyatomic projectiles*. For polyatomic bombardment one is examining relative yields and the mechanisms for vastly different yields. This scenario is a perfect match for MD simulations.
- *Cluster formation from atomic solids*. Obtaining quantitative yields of clusters requires an interaction potential that describes the chemistry of bonding reasonably well. Moreover, as described below, it is important to include unimolecular decay during the flight[52] to the detector and the resulting changes in the yields and energy distributions. With care, however, once can learn some aspects of cluster formation and probabilities.

- *Dissociation reactions of organic molecules*. Determining which organic molecules are directly dissociated during the collision cascade can be reliably calculated with the Brenner potential. Determining the precise dissociation products, on the other hand, is more challenging.
- *Rearrangement reactions of organic molecules*. As discussed below, it is possible to estimate with the Brenner potential that molecules that have ejected have sufficient energy to rearrange and unimolecularly decay during the flight to the detector. The potential is not sufficiently good, however, to predict the reaction products.
- *Reactions between organic molecules*. The Brenner hydrocarbon potential was developed to describe H abstraction reactions. Other reactions were not built into the potential and should thus be assessed for chemical sensibility. Mechanistic pathways proposed in the simulations may be sufficiently prevalent or are so chemically intuitive that they cannot be ignored. For example, using the Brenner potential in MD simulations of diamond surfaces, a β-scission reaction for carbon insertion into the surface dimer bond was predicted.[53] Although the mechanism was speculative at the time, the prediction has been shown to be quite feasible by traditional organic chemistry methodology on small molecule analogues of the diamond surface structure.[54,55]
- *Point of origin on the surface*. The position in the system relative to the primary particle impact at which some event such as ejection, fragmentation or reaction occurs is easy to determine with MD simulations. More discussion on this topic is included in the chapter by Delcorte.[5]
- *Time of an event*. The time at which an event such as ejection occurs is straightforward to determine with MD simulations. An example of time of ejection is given later in this chapter.
- *Range.* Calculating the range of deposition of high-energy particles requires very large crystals and is better treated with collision cascade theory.[4]
- *Diffusion*. Diffusion generally occurs on the time scale of microseconds to seconds and thus cannot be determined with straightforward MD simulations. Extending the time scale of MD simulations is a current topic of study for several groups.
- *Final damage and mixing*. The final bonding configurations of a damaged site and the intermixing of several elements is highly dependent on the quality of the chemical part of the interaction potential. Mixing may also have a contribution from diffusion, a long time scale process. A nice example of damage in solids, related to carbon erosion by hydrogen bombardment in divertor materials of fusion reactors, is given in recent papers from the Nordlund group.[56,57] In these studies the primary particle energies are low, strong bonds inhibit significant diffusion and the potential (Brenner CH) mimics reasonable chemistry.
- *Dynamic SIMS*. To model dynamic SIMS, one must have a set of initial configurations that represent the solid after it has been struck by previous primary particles. To obtain these configurations, one should run a simulation until all the processes in the solid stop and then bombard with another primary particle. These

simulations thus combine the challenges of diffusion (long time scale) and mixing (quality of interaction potential). Moreover, a huge crystal would be needed. Some attempts, however, have been made in this direction[58] and with care some concepts can be learned.

10.2.10 Getting started doing simulations

How does one start doing simulations? My best advice is to collaborate with a group already actively involved doing simulations. I certainly would not attempt to start doing SIMS experiments without proper guidance from an experienced SIMS researcher. I have tried to reference work from all the current groups modelling SIMS experiments in this chapter. Another source of references are the proceedings from biennial meetings on Computer Simulations of Radiation Effects in Solids.[59–61] Finally, in late 1999 we wrote an *Accounts of Chemical Research* article in which we tried to reference all papers at that time dealing with sputtering of organic molecules.[62]

10.3 Examples of results

What are the expectations for the results from the MD simulations? Which pieces of information can be trusted and which should be held suspect? Certainly, these are valid questions to ask of any simulation, or experiment for that matter. Ultimately the answers to these questions lie in comparisons of results from the simulations to existing experimental data and predictions from the simulations that are tested by further experiments. The simulations can be useful even if they only suggest to the experimentalist a new way of thinking about the events that might happen during a bombardment event.

There have been numerous comparisons of results of MD simulations to experimental results. The focus here is on issues directly relevant to ToF-SIMS. Thus, we will omit discussions of energy and angular distributions of metal systems[11,51] for which very detailed and quantitative comparisons have been made. As mentioned above, we did recently write an article for *Accounts in Chemical Research*[62] on a similar topic, thus we are attempting to make this article have a different focus. Topics to be discussed include interpreting the entire mass spectrum, ejection of upright chains and clipping, reactions between molecules, cooperative uplifting, megaevents and cluster/fragment distributions.

10.3.1 Mass spectra

A wonderful objective would be to predict experimental mass spectra for any molecule and system of choice. The challenges in doing so are many-fold. First, there is the nagging issue of ionisation. Second, realistically running MD simulations for more than a few ps is computationally intensive and running them for more than a few ns introduces numerical errors. The flight time to the experimental detector is generally several μs. Finally, to model a system of choice one needs the appropriate interaction potential. One can use, however, the simulations to understand portions of the spectrum. For example, in

Reference 2 and summarised in the Introduction, several aspects of the positive and negative spectra from alkanethiol overlayers on metal substrates have been explained. Similarly, we have interpreted portions of the polystyrene spectrum[63] and spectra of short hydrocarbon chains.[64] Through the understanding of portions of the spectra, general mechanisms and considerations relevant to interpreting mass spectra have been elucidated. Several of these are given below.

10.3.2 Upright molecules—fragmentation vs molecular ejection

One general class of systems examined is upright molecules. These include alkanethiols[2] as shown in Figure 2, ethylidyne type species as shown in Figure 4 or 6(a),[65,66] pyridine[67] and even the phenyl group of a polystyrene oligomer.[63] These species are easy targets to be hit by fragments from other molecules. If the molecule is weakly bound to the substrate,[66] then it is possible for the molecule to be ejected intact as shown in Figure 6(b). On the other hand, if the molecule is tightly bound to the substrate, then fragmentation tends to occur[2,65,66] as shown in Figure 6(c). Clipping of the tops of chains to produce fragments is invoked in the Introduction to explain the presence of the $C_nH_{2n+1}^+$ ions in the mass spectrum of alkanethiols on Au surfaces. Clipping events are shown in pink in Figure 2.

The concept of intact ejection as a function of binding energy to the substrate has been examined experimentally for peptides on polystyrene beads.[68] When the peptide is covalently bound to the bead, no molecular signal is observed. When the bond is severed with trifluoroacetic acid such that the molecule is physisorbed to the bead, then the parent molecule signal is intense.

The ejection of molecules with multiple contact points to the surface leads naturally into the discussion of megaevents and stability of clusters. Thus, the discussion of reactions between molecules is presented next.

10.3.3 Reactions between molecules

One prediction from the simulations that surprised us at the time is that fragments from one molecule can react with another molecule to produce a new molecule.[3] Although many variations exist, the two main abstraction mechanisms seen for the formation of H_2 are shown in Figure 7. In the predominant mechanism, Scheme 1, a H atom is emitted when the C_2H_3 molecule on the right is hit by either an energetic Pt atom, an Ar atom or a CH_x (x = 0–3) fragment. Once emitted, this H atom is propelled in the direction of a H atom on an undisturbed C_2H_3 molecule. This results in the formation of a H–H bond and the breaking of a C–H bond. Scheme 2 shows an intriguing mechanism in which a C_2H_3 molecule is bumped such that one of its H atoms interacts with a H atom on the neighbouring C_2H_3 molecule. H_2 is formed, and two C–H bonds are broken. Our simulations on organic systems consistently show large amounts of molecular H_2 and the vast majority arises from abstraction reactions. In a similar process,[65] a CH_3 fragment can abstract a H atom from another molecule to form CH_4. The abstraction process can also occur between a fragment such as C_7H_6 from a polystyrene molecule and another H atom

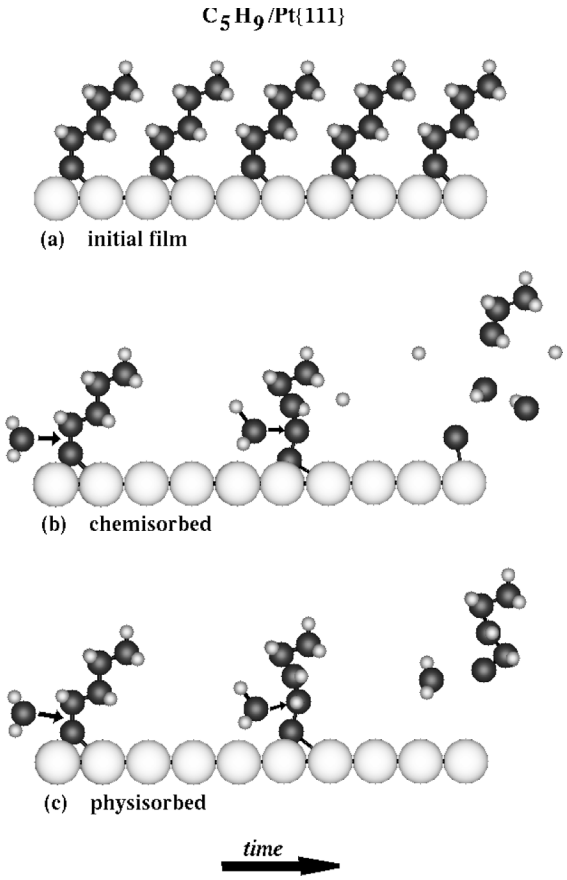

Figure 6. C_5H_9 bound in fcc threefold site on Pt{111}: (a) initial array; (b) scenario for ejection of the C_3H_7 fragment from C_5H_9 film bound by 2.70 eV (chemisorbed) on Pt{111}; (c) scenario for ejection of the C_5H_9 molecule from C_5H_9 film bound by 0.60 eV (physisorbed) on Pt{111}. In (b) and (c), the time progression is from left to right across the crystal. See text for an explanation of the collisional events. The large light grey spheres represent Pt atoms, the medium-sized dark spheres represent C atoms and the small spheres represent H atoms. Reprinted from R.S. Taylor, C.L. Brummel, N. Winograd, B.J. Garrison and J.C. Vickerman, *Chem. Phys. Lett.* 233, 575 (1995), with permission from Elsevier Science.

on the same molecule.[63] The C_7H_7 species formed is also observed in experimental spectrum[69] and cannot be explained as a direct fragmentation species nor is it an obvious rearrangement species. Similarly, a C_5H_{11} species shown in blue in Figure 2 abstracts an H atom from another molecule to form C_5H_{12}. Finally, reactions between free CH_3 and H radicals have been observed in the near surface region in the simulations.[65]

The ultimate importance of reactions between fragments and other molecules is not yet resolved. The molecular systems do have atoms close together and there are many fragments created in the bombardment event. Reactions must be occurring. For another

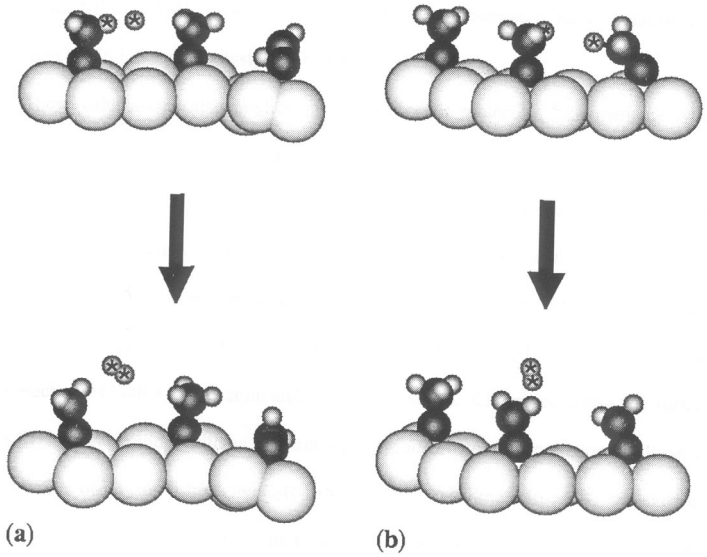

Figure 7. Two pathways found for H abstraction. The light gray, black and white spheres represent the Pt, C and H atoms, respectively. The H atoms that eventually form the H_2 molecule are marked with stars. In Scheme 1, the middle C_2H_3 is out of the plane of the reacting C_2H_3 molecules and does not enter into the H abstraction reaction. See the text for a description of the details. Reprinted with permission from Reference 3. Copyright 1994 American Chemical Society.

type of system, namely ionic solids there is strong experimental evidence that reactions between ligands are a major factor in determining the spectrum.[70]

10.3.4 Cooperative uplifting and molecules with multiple contacts to the surface

The predominant ejection mechanism for molecules with multiple contact points to the surface is one in which several substrate atoms hit different parts of the molecule, resulting in cooperative uplifting of the intact molecule.[40,47,62,63,71,72] The imparted upward energy to the molecule thus arises from several gentle collisions rather than a collision with one energetic substrate atom. A secondary process is one in which predominantly a single substrate atom ejects the adsorbed molecule. Ultimately, though, we believe that the cooperative uplifting mechanism with many substrate atoms participating is responsible for the ejection of large molecules.

10.3.5 Megaevents, large molecule and cluster ejection

In simulations of sputtering of Cu single crystals, Don Harrison identified certain trajectories that he and Peter Williams termed megaevents.[6] There is now a recurring theme in many simulations that these megaevents are important for the ejection of large molecules as well as large clusters of atoms.

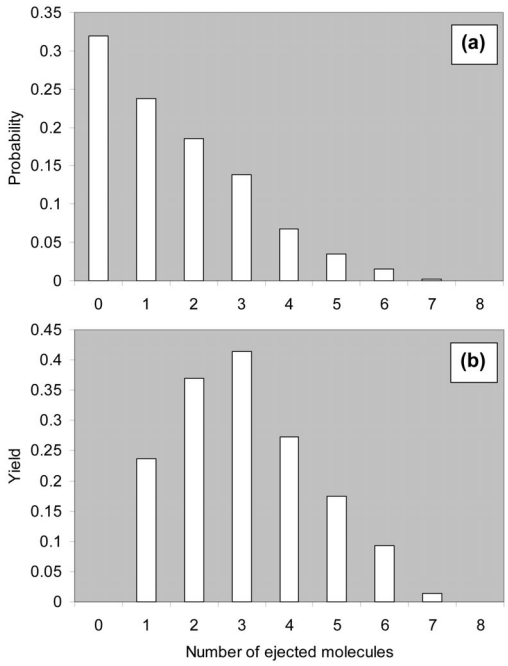

Figure 8. (a) Probability distribution of intact molecule ejection for 5 keV Ar bombardment of polystyrene tetramers on a Ag(111) surface. (b) Associated yield distribution. Figure adapted and reprinted with permission from Reference 47. Copyright 2000 American Chemical Society.

10.3.5.1 Megaevents

In both experiments and simulations, measurable quantities are averages over many primary particle collisions on the substrate. Depending on the aiming point, the action and subsequent yield of ejected species can differ significantly. One means of examining the diversity of action is to plot the number of aiming points that give rise to a specific yield. Such a distribution is shown in Figure 8(a) for a system of polystyrene tetramers adsorbed on a Ag surface bombarded by 5 keV Ar.[47] Depending on the particular aiming point anywhere from zero to eight molecules can eject from one primary particle hit. The most probable number of molecules ejected is zero. From this perspective, the events in which three or more molecules eject do not appear important. The critical quantity, however, is the contribution of the various trajectories to the molecular ejection yield as shown in Figure 8(b). The events in which three or more molecules eject contribute over half of the total molecular yield. Strictly speaking, Harrison and Williams originally used the word megaevent to mean only the events that give rise to ~5% of the yield. I am being a little more generous in the definition.

A series of snapshots from a megaevent for the polystyrene tetramer on Ag system is displayed in Figure 9. This particular trajectory sputters six molecules, 24 Ag atoms, 24

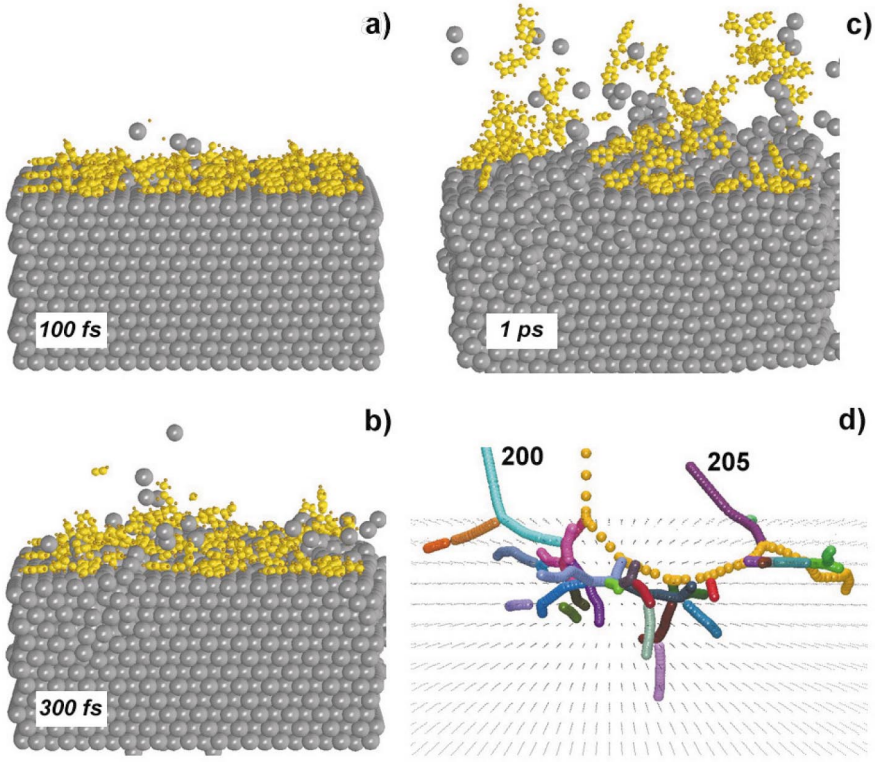

Figure 9. Time evolution of a high-yield trajectory under 5 keV Ar bombardment. (a) 100 fs; (b) 300 fs; (c) 1000 fs. (d) Collision tree showing the high energy part of the cascades after 100 fs for the same trajectory (E). The incident particle is represented by yellow spheres. See text for details. Reprinted with permission from Reference 47. Copyright 2000 American Chemical Society.

Ag atoms incorporated in clusters and numerous organic fragments. The mass of each molecule (fully tritiated as described above) is 559 amu. The total mass sputtered by the 5 keV Ar projectile in this one collision cascade is over 10,000 amu. Computationally we are able to put two hexadecamers of polystyrene on the surface and start the trajectory with the same high action.[47] In this case, two molecules with over 2000 amu each are ejected. Snapshots of this motion can be found in Reference 47 and in the chapter by Delcorte.[5]

Megaevents or high-yield trajectories are also important for large metal clusters.[73] Cluster distributions as shown in the chapter by Urbassek[4] extend experimentally to at least 60 atoms.[74] Clearly, if clusters containing over 60 atoms eject, then at least that number of atoms must eject in one primary particle incidence on the substrate. Of note is that typical sputtering yields are 1–10, thus the high yield events have a low probability of occurring just as shown in Figure 8(a) for molecule ejection.

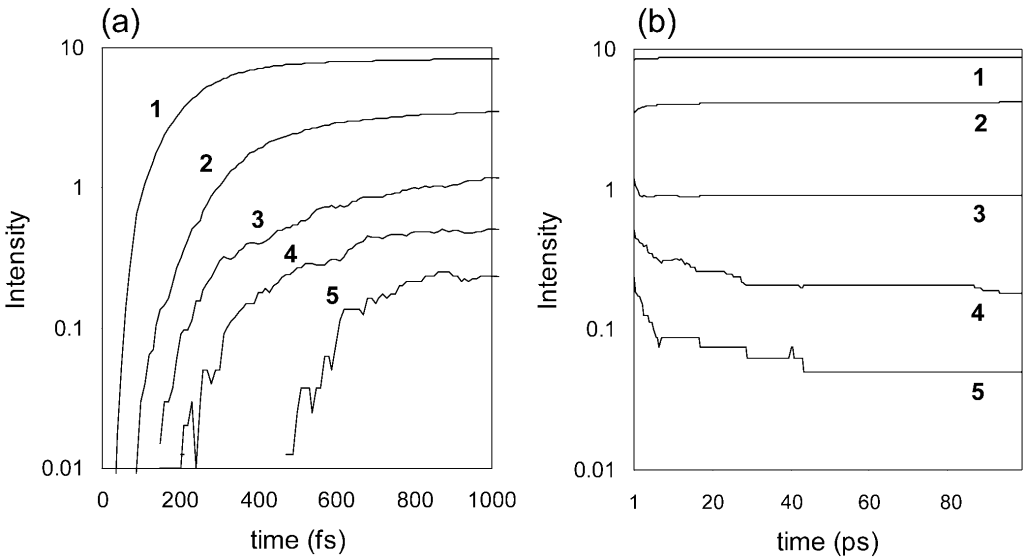

Figure 10. Yield of Cu_n, n = 1,5, vs time. (a) During the collision cascade. (b) After the collision cascade. Reprinted from T.J. Colla, H.M. Urbassek, A. Wucher, C. Staudt, R. Heinrich, B.J. Garrison, C. Dandachi and G. Betz, *Nucl. Instrum. Methods. Phys. Res. B* 143, 284 (1998), with permission from Elsevier Science.

10.3.5.2 Computational challenges

Simply stated, trajectories that are megaevents require more computational resources. First, the crystal size required for a trajectory in which many particles eject is greater than if nothing ejects. Unfortunately, we do not know ahead of time which aiming points on the surface will be megaevents so we generally use the same size crystal for all trajectories. Second, the time of emission of large molecules or clusters is longer than for atoms. This effect is shown in Figure 10(a) where the intensity of Cu_n for $n = 1 \rightarrow 5$ is plotted vs time in the trajectory. The atoms typically eject first, then dimers and finally the larger clusters. As shown in Figure 8(a), the probability of any given aiming point being a megaevent is a low probability event. Thus, more trajectories must be calculated in order to find the ones of interest. Currently, calculating distributions including the very large clusters for metal systems is a computational challenge, and as shown in Table 3, trajectories on metal systems are relatively fast to compute.

10.3.5.3 Physics of megaevents and molecular ejection

Over the years, especially before we could do large-scale simulations, several conceptual models for sputtering were delineated. As discussed in the chapter by Urbassek,[4] Sigmund's theory concerns linear collision cascades.[75] There was recognition, however, that there might be regimes in which the atoms do not collide in pairs. Words used to describe these regimes included thermal spikes[76–79] and megaevents.[6,80] In particular, there

are many models that invoke collective motions that give rise to the ejection of large molecules and clusters of atoms.[81]

A clear situation in which collective effects *always* dominate is laser ablation as is applicable for matrix-assisted laser desorption/ionisation (MALDI).[82,83] In this case, there is a laser fluence regime in which a large nearly contiguous volume of material is removed. For laser conditions typical of UV MALDI, the physics driving ablation is an overheating of the material, followed by an explosive vaporisation into individual molecules and clusters of molecules. For pulses shorter than the mechanical relaxation time of the material, spallation or mechanical cracking that gives rise to the removal of material can also occur.

In order to try and decipher whether sputtering clearly falls into the same category of collective motion as laser ablation/MALDI, we analysed the simulations of the polystyrene tetramer using graphical *lean-on* trees[47] as shown in Figure 9(d). Our objective is to identify the genesis of the action giving rise to massive ejection. The lean-on tree shows a summary of the high-energy action in the first 100 fs of the trajectory. The aim is to show the successive positions of the moving atoms as a function of time in a single plot. Atoms are shown if their energy exceeds 100 eV. For clarity, the atoms are turned off if their energy falls below 25 eV. Trajectories such as the one shown in Figure 9(d) that give rise to large numbers of particles ejecting are ones in which the energy of the primary particle is rapidly and almost equitably partitioned among many substrate atoms in the near surface region.[47] If the energy partitioning is too far below the surface or too much energy is channelled deeper into the substrate, not as much material ejects. Subsequent to the rapid partitioning of the energy of the primary particle at ~200 fs, the Ag atoms in the top two to three surface layers are moving upward in concert and the Ag atoms in the bottom few layers are moving downward towards the bulk of the sample. The effect of these initial high energy motions and concerted upward motions of the top few layers starts to eject species at later times as shown in Figure 9(b,c).

What nomenclature do we use for events such as shown in Figure 9 to describe correctly what is happening. Is the motion a thermal spike? Betz has shown that a Maxwell–Boltzmann distribution of velocities develops after ~1 ps in trajectories in which large metal clusters eject.[84] The troublesome connotation associated with the word thermal is the concept of equilibrium. Can a true equilibrium be reached in 1–2 ps? In fact, our pictures show a clear bifurcation with atoms in the top few layers preferentially moving upwards and the atoms in the layers below moving downward. This observation would argue against any thermal equilibrium since the upward and downward motions are not randomly mixed. Is the motion truly collective? Certainly as mentioned above there does appear to be some level of correlation among the atomic motions. If the correlation exists, it is not on the same length scale as in laser ablation or MALDI,[82,83] nor are there strong correlations in all primary particle collision cascades. In fact, we have speculated[47] that the longer length scale of the correlated motion in laser ablation is the reason for larger mass molecules (~100s kDa) being detected in MALDI vs in SIMS (~10s kDa).

For sputtering of systems of metal supports with atomic projectiles, there is clearly a variety of types of motion induced by the primary particle. Some incident particle trajectories involve the primary particle finding a channel and moving through the target without ejecting anything. There are also trajectories where there is tremendous motion as shown in Figure 9. Moreover, there is a continuum of action in between these two extremes. For now we prefer the word megaevents to describe these trajectories in which there is a massive amount of material removed. These events are part of the continuum of actions that can occur due to an energetic primary particle striking a substrate and special physics does not have to be invoked.

10.3.6 Molecules and clusters, stable or not?

In order to make comparisons between the calculated yields and the experimental values, one must evaluate the survivability of the groups of atoms for tens of μs, i.e. the average experimental delay between molecule ejection and detection. In the simulation, we use a simple approach to determine whether a group of atoms is a molecular cluster. We first separate out the centre-of-mass kinetic energy and then calculate the kinetic energy relative to the centre-of-mass. The sum of the relative kinetic energy and potential energy is then used to determine if we have a molecule or not. If the sum is negative, then we define the group of atoms to be a cluster or molecule. This definition of a molecule, however, is only rigorously valid for dimers. For triatomic and larger species, there is the possibility that a group of atoms above the surface might unimolecularly dissociate as shown in Figure 4 for $HCCH_2$ going to HCCH + H. Since there is correlation between the internal energy and the centre-of-mass kinetic energy, unimolecular dissociation reactions have an effect on the measured kinetic energy distribution as well as the yields. Therefore, it is crucial to develop an operational method to determine which molecules are stable and which ones are not with respect to the longer time scale of the experiment.[71,63,65]

10.3.6.1 Determining stable molecules

In the best situation, one can use MD simulations to evaluate which groups of atoms will dissociate and then determine the final products, kinetic energies and internal energies. Operationally at the end of the collision cascade, one continues integrating the equations of motion for the particles above the surface.[52] The substrate atoms are omitted in order to speed up the calculation. The results of such a calculation for Cu clusters are shown in Figure 10(b). Obviously, the intensities of the larger clusters decrease and the intensities of the Cu and Cu_2 species increase. As an aside, the observation that many of the big clusters unimolecularly dissociate before reaching the detector makes finding aiming points that give rise to *stable* big clusters even more challenging and time consuming.

One can semi-reliably determine the unimolecular dissociation of metal clusters with MD simulations. The interaction potential predicts that mostly individual atoms and some diatomic molecules are the dissociation products. This description is probably reasonable. The dissociation channel is straightforward and does not involve complex and slow to occur rearrangement events. Thus, the lifetimes are less than hundreds of ps.

As much we might want to follow the dissociation pathways of organic molecules as they traverse the microseconds it takes them to reach an experimental detector, such a MD simulation is currently impossible for several reasons. First, the currently available potential is not sufficiently flexible to reproduce all the possible dissociation pathways. Second, even if the potential were adequate, activation barriers in the dissociation pathways produce lifetimes beyond the capability of the MD method. Third, for molecules with a large number of atoms, the time for the energy to localise in the dissociation pathway can also be long

Although the stability of organic molecules cannot be computationally verified for the reasons quoted above, the simulation provides us with a quantitative evaluation of the internal energy of sputtered species. Because the lifetime of metastable species depend directly on their internal energy, determining the survivability of a sputtered molecule can be achieved by comparing its internal energy to a realistic energy threshold for unimolecular dissociation for the given time-of-flight of the species to the detector.[63] Such an energy threshold can be deduced from experimental *dissociation rate* versus *internal energy* curves.[85–87] These curves, however, are not available for all the fragments ejected in the sputtering process. Alternatively, the classical Rice–Ramsberger–Kassel (RRK) theory, in which the molecule is represented by a set of *s* oscillators, provides a reasonable approximation of the relation between internal energy (E_{int}) and lifetimes (τ). In this treatment, the rate of dissociation of the molecule, equal to the inverse of the average lifetime τ, is given by Equation 4

$$rate = 1/\tau = A(1 - E_0/E_{int}\mathrm{A})^{s-1} \quad (4)$$

where A is a proportionality constant ($A \approx 10^{13}$ s^{-1}), E_0 is the critical energy for dissociation and *s* is the number of vibrational modes in the molecule. A major advantage of using the RRK theory is that Equation 4 can be easily applied to all the sputtered species as an automated part of the data analysis. The main drawback of this method, also related to its simplicity, is the limited accuracy of the results. A more accurate treatment would require the use of quantum theory, which is beyond the scope of our current abilities. Another limitation of the RRK method is that the identity of the dissociation products cannot be ascertained.

In practice, the combined use of MD simulations and RRK theory shows that several convoluted factors are involved in estimating the number of molecules that reach the detector. Larger molecules and fragments tend to have larger internal energies.[63–65] In parallel, they have more internal degrees of freedom, thus the internal energy they can have without dissociating is larger. Finally, the time-of-flight to the detector is larger for more massive molecules, thus the internal energy they can tolerate is reduced accordingly.

10.3.6.2 Influence on mass spectra

Given the prescription described above the corrected mass spectrum for polystyrene tetramers on Ag is less intense in general but there is not a clear dependence of the relative intensity change on the mass of the sputtered species,[63] in contrast with the use of a constant energy threshold as used in our initial studies[2,65] For instance, with the RRK-based threshold, 58% of the C_3H_2 (38 amu), 52% of the C_6H_5 (77 amu), 49% of the C_8H_9 (105 amu) and 69% of the $C_{12}H_{17}$ (161 amu) survive to the virtual detector. Due to the relatively high threshold for dissociation of the entire PS tetramer (28 eV), the intensity of this peak in the corrected mass spectrum is not significantly reduced (94% of its initial value).

10.3.6.3 Influence on kinetic energy distributions

To calculate kinetic energy distributions (KEDs) accurately, the molecules that unimolecularly dissociate must be properly treated. For the Cu system where the dissociation products are known, the effect on the Cu atom distribution has been calculated.[52] The larger clusters that dissociate preferentially yield Cu atoms with low kinetic energies. The net change from a kinetic energy distribution calculated with the intensities at 1 ps vs 10 ps is that the peak in the energy distribution shifts to a lower value and it increases in intensity.

Insight into the basic shape of the KED *of molecules* has been provided by the MD simulations. Atomic KEDs have been reasonably well described over the years by a Thompson distribution.[88] Specifically, there is a peak in the distribution and the high-energy tail falls off as E^{-2}. In a recent study using a postionisation technique, the KED of neutral benzene molecules sputtered from a Ag surface was measured.[89] The high-energy tail of the benzene molecules falls off much faster than E^{-2}. Complementary MD simulations also show that the high-energy tail falls off quite quickly.[71] The MD simulations clearly show molecules struck with sufficient energy to possibly sputter with high kinetic energies tend to dissociate. The lack of a high-energy tail in the KEDs of molecules is due to dissociation of molecules. There is still a collision cascade and no thermal process needs to be invoked. The comparison of the corrected KEDs as a function of mass for the polystyrene system have been delineated elsewhere.[63] The corrections are important in obtaining good agreement with experimental data. As a caveat, though, we still cannot adjust the distribution of the fragment species of the organic species as is shown for Cu and Cu_2 yields shown in Figure 10(b).

10.4 Forefront areas

Where do we go next? What critical issues need to be addressed? First, thick organic films, larger kinetic energies of the primary particle and polyatomic particle bom-

bardment *merely* require some more computer power. These areas are discussed more below. Second, empirical interaction potentials appropriate for sputtering simulations do not exist for systems containing three or more elements such as C, H, O and N; systems containing metal atoms with organic ligands; or insulators such as SiO_2. Consequently, we may be missing some important classes of events. Unfortunately, the interest in generating empirical potentials has waned over the years. Third, there is the old nemesis, ionisation! I am not optimistic that in the near future we will be able to develop a first principles computational approach to ionisation. Rather, as specific experimental results appear that demand the inclusion of ionisation effects, a modelling approach may be appropriate.[18,19]

Organic, biological and polymeric solids represent a large fraction of the samples of interest to the ToF-SIMS community. Open issues include the sampling depth of molecules ejected, how fragments occur, how much reaction between molecules takes place, how much damage is created and what is the fundamental nature of the collision cascade. An interaction potential[36] is now available to allow us to model molecular hydrocarbon films and we have started efforts in this direction.[61] Molecular solids, however, consume enormous amounts of computer time as the potentials are longer ranged and more forces need to be evaluated, H atom motions require smaller integration time steps and the cohesive energies tend to be smaller than metals thus larger crystal sizes than currently being used are required. Coupled with the desire to move towards organic solids is the realisation that there may be some effect of the incident particle energy.[47,63] There may be mechanisms essential to understanding ejection processes at higher incident energies that are not present at lower incident energies. Typical ToF-SIMS incident energies are 10–25 keV, at least a factor of five greater than we typically use in the simulations. The higher energy incident particle may travel farther into the sample and do less sputtering. On the other hand, it may unleash enormous megaevents.

One of the fascinating experimental observations is that in some instances polyatomic incident particles can increase greatly the useful yield over that with atomic projectiles.[90,91] The enhancement is especially apparent for molecular solids where the yield can increase by a factor of ~1000 in going from atomic C to polyatomic C_7 incident projectiles.[91] Several groups have modelled polyatomic bombardment of metal substrates[92] and we have modelled polyatomic bombardment of organic overlayers on metal and silicon substrates.[93,94] One interesting conclusion from our simulations is that the openness of the substrate is a critical factor for the polyatomic projectile to be effective. On the silicon substrate, SF_5 is able to penetrate beneath the top layer of the surface and break into fragments. The breakup of the SF_5 cluster within the lattice initiates collision cascades that lead to substrate atoms hitting organic molecules from below and lifting them off the surface. In contrast, when SF_5 strikes a Cu surface, the polyatomic projectile fragments at the top metal surface and is thus less effective at sputtering molecules. Examining polyatomic bombardment of organic solids by the MD simulations is obviously of high priority given the experimental interest.

10.5 Successes of MD simulations for understanding sputtering

Over the years, MD simulations have become, in my biased opinion, the predominant method for understanding sputtering. When Don Harrison started his simulations in the 1960s, there was virtually no data to test the accuracy of the simulations. During the next decades, the experimental data became sufficiently sophisticated that analytic theories could not be used and MD simulations took over. Below is a partial list of the successes of MD simulations in providing insight into and quantitative comparisons to experimental sputtering results.

- Clusters of metal atoms do not necessarily arise from contiguous atoms on the surface.[95]
- Atoms sputtered from metal surfaces eject predominantly from the surface layer and not from deeper in the bulk.[96]
- Angular distributions of adsorbed atoms and molecules reflect the bonding geometry on the surface.[97]
- Energy and angular distributions from single crystal metal and semiconductor surfaces can be quantitatively described.[51]
- Collisions in the near surface region contribute to excited state formation.[18]
- Cooperative uplifting gives rise to the ejection of molecules.[67]
- Megaevents do occur[6] and may be responsible for the ejection of the very large molecules.[47]
- Clipping of the tops of alkane chains is responsible for fragments such as $C_nH_{2n+1}^+$.[2,65,66]
- Reactions can occur between molecules.[3]
- Variations in widths of kinetic energy distributions with fragment size for polystyrene oligomers can be explained in one corrects for unimolecular decay during the flight to the detector.[63]

10.6 Acknowledgements

More years than perhaps I wish to acknowledge have been spent modelling sputtering. I would like to thank Nick Winograd for piquing my interest in 1976 about the formation mechanisms of metal clusters that eject in SIMS. Nick has been a continuous partner in these studies since then. The late Don E. Harrison inspired us as to the possibilities of modelling sputtering and to the realities of acceptance of our computer simulations results by others. Unfortunately, Don did not live to see MD simulations become the backbone of the theoretical efforts for understanding sputtering. Don was the person that gave me my first computer code for the sputtering simulations. Many of Don's concepts for handling situations in the simulations peculiar to sputtering are still present in our current code, SPUT93, written by David Sanders.

Numerous students, postdocs and collaborators of Nick's and mine have contributed to our understanding of sputtering of organic molecules via computer simulations. These people include Reema Chatterjee, Arnaud Delcorte, Kristin Krantzman, Susanna

Liu, Zbigniew Postawa, Ramona Taylor and John Vickerman. Thanks also go to many other people, too numerous to mention, with whom I have collaborated over the years. Thanks go especially to my ex-student Don Brenner, now a Professor at North Carolina State University, for developing the potential to describe hydrocarbon reactions. Steven Stuart and Judith Harrison have provided us with the AIREBO potential, which will take us to the next generation of simulations.

The financial support of the National Science Foundation through the Chemistry Division, the CRIF program, and the MRI program as well as the Office of Naval Research are gratefully acknowledged. Additional computational resources were provided in part by the IBM Selected University Resource Program and the Center for Academic Computing of Penn State University. Further information from our simulations including publications, graphics and animations can be obtained from web page, http://galilei.chem.psu.edu/.

10.7 References

1. (a) J.C. Vickerman, D. Briggs and A. Henderson, in *The Static SIMS Library*. SurfaceSpectra, Manchester, p. 2:3. 1–4 (1998); (b) J.C. Vickerman, D. Briggs and A. Henderson, in *The Static SIMS Library*. SurfaceSpectra, Manchester, p. 3:3. 29 (1998).
2. K.S.S. Liu, C.W. Yong, B.J. Garrison and J.C. Vickerman, *J. Phys. Chem. B* **103,** 3195 (1999).
3. R.S. Taylor and B.J. Garrison, *J. Am. Chem. Soc.* **116,** 4465 (1994).
4. H.M. Urbassek, chapter in this volume
5. A. Delcorte, chapter in this volume
6. D.E. Harrison, Jr, *Crit. Rev. Sol. State and Mat. Sci.* **14,** S1 (1988).
7. H.M. Urbassek, *Nucl. Instrum. Methods B* **122,** 427 (1997).
8. B.J. Garrison, N. Winograd and D.E. Harrison, Jr, *J. Chem. Phys.* **69,** 1440 (1978).
9. N. Winograd and B.J. Garrison, in *Ion Spectroscopies for Surface Analysis*, Ed by A.W. Czanderna and D.M. Hercules. Plenum Press, New York, p. 45 (1991).
10. B.J. Garrison, *Chem. Soc. Rev.* **21,** 155 (1992).
11. D.N. Bernardo, R. Bhatia and B.J. Garrison, *Comput. Phys. Commun.* **80,** 259 (1994).
12. R. Smith, M. Jakas, D. Ashworth, B. Oven, M. Bowyer, I. Chakarov and R. Webb, in *Atomic and ion collisions in solids and at surfaces*, Ed by R. Smith. Cambridge University Press, Cambridge, UK (1997).
13. J.B. Gibson, A.N. Goland, M. Milgram and G.H. Vineyard, *Phys. Rev.* **120,** 1229 (1960).
14. W.L. Gay and D.E. Harrison, Jr, *Phys. Rev.* **135,** 1780 (1964).
15. U. Fano and W. Lichten, *Phys. Rev. Lett.* **14,** 627 (1965).
16. M.H. Shapiro and J. Fine, *Nucl. Instrum. Methods B* **44,** 43 (1989).

17. J.J. Vrakking and A. Kroes, *Surf. Sci.* **84,** 153 (1979).
18. N. Winograd, M. El-Maazawi, R. Maboudian, Z. Postawa, D.N. Bernardo and B.J. Garrison, *J. Chem. Phys.* **96,** 6314 (1992); M. El-Maazawi, R. Maboudian, Z. Postawa, N. Winograd and B.J. Garrison, *J. Chem. Phys.* **97,** 3846 (1992).
19. M.L. Yu and N.D. Lang, *Phys. Rev. Lett.* **50,** 127 (1983).
20. The nuclear–nuclear repulsion terms are also included in the interaction potential.
21. There is considerable effort by several researchers to develop approaches for performing direct force evaluations from electronic structure calculations. At this stage, however, the computer time requirements are too extensive to use thousands of atoms and run for as long a time as is needed for sputtering calculations.
22. This prescription for developing an empirical potential sounds quite straightforward. In fact, figuring out a functional form that is close to the solution to the Schrödinger equation takes a certain amount of talent. Considerable experimental data is required. Constructing empirical potentials is a major research effort.
23. The pairwise additive assumption works quantitatively well for systems such as liquid and solid Ar in which there are primarily van der Waals interactions.
24. Several years ago, we wrote a review article summarising and referencing many of the available many-body potentials: B.J. Garrison and D. Srivastava, *Ann. Rev. Phys. Chem.* **46,** 373 (1995).
25. S.M. Foiles, M.I. Baskes and M.S. Daw, *Phys. Rev. B* **33,** 7983 (1986).
26. T.J. Raeker and A.E. DePristo, *Intl. Rev. Phys. Chem.* **10,** 1 (1991).
27. C.L. Kelchner, D.M. Halstead, L.S. Perkins, N.M. Wallace and A.E. DePristo, *Surface Sci.* **310,** 425 (1994).
28. F.H. Stillinger and T.A. Weber, *Phys. Rev. B* **31,** 5262 (1985).
29. J. Tersoff, *Chem. Phys. Rev. B* **37,** 6991 (1988).
30. D.W. Brenner, *Phys. Rev. B* **42,** 9458 (1990).
31. B.J. Garrison, P.B.S. Kodali and D. Srivastava, *Chem. Rev.* **96,** 1327 (1996).
32. N.L. Allinger, K. Chen and J. Lii, *J. Comput. Chem.* **17,** 642 (1996).
33. T.A. Halgren, *J. Comput. Chem.* **17,** 490 (1996).
34. W.L. Jorgensen, D.S. Maxwell and J. Tirado-Rives, *J. Am. Chem. Soc.* **118,** 11225 (1996).
35. W.D. Cornell, P. Cieplak, C.I. Bayly, I.R. Gould, K.M. Merz Jr, D.M. Ferguson, D.C. Spellmeyer, T. Fox, J.W. Caldwell and P.A. Kollman, *J. Am. Chem Soc.* **117,** 5179 (1995).
36. S.J. Stuart, A.B. Tutein and J.A. Harrison, *J. Chem. Phys.* **112,** 6472 (2000).
37. The integrator given by Equation 3 is for displaying the essential idea of numerical integration clearly and is not one that should be used in simulations as it is unstable.
38. I.M. Torrens, *Interatomic Potentials*. Academic Press, New York (1972).
39. D.J. O'Connor and R.J. MacDonald, *Radiation Effects* **34,** 247 (1977).
40. R. Zaric, B. Pearson, K.D. Krantzman and B.J. Garrison, *Int. J. Mass Spec. Ion Proc.* **174,** 155 (1998).
41. M. Karplus, R.N. Porter and R.D. Sharma, *J. Chem. Phys.* **104,** 3259 (1965).

42. J.S. Burnham, D.E. Sanders, C. Xu, R.M. Braun, S.H. Goss, K.P. Caffey, B.J. Garrison, and N. Winograd, *Phys. Rev. B* **53,** 9901 (1996); S.H. Goss, G.L. Fisher, P.B.S. Kodali, B.J. Garrison and N. Winograd, *Phys. Rev. B* **59,** 10662 (1999); R. Blumenthal, K.P. Caffey, E. Furman, B.J. Garrison and N. Winograd, *Phys. Rev. B* **44,** 12830 (1991).
43. B.V. King, C. Zimmerman, D.E. Riederer, S.W. Rosencrance, B.J. Garrison and N. Winograd, *Rapid Commun. Mass Spectrom.* **12,** 1236 (1998).
44. S.W. Rosencrance, N. Winograd, B.J. Garrison and Z. Postawa, *Phys. Rev. B* **53,** 2378 (1996).
45. By temperature dependence, in this case we refer to the effect of a Maxwell–Boltzmann distribution of positions and velocities. Temperature can also cause a change in structure of the system. For example, at low temperatures ethylene adsorbs molecularly on Pt. At room temperature, it converts to the ethylidyne structure. These types of temperature effects can be model by choosing both configurations for the simulations.
46. R.S. Taylor and B.J. Garrison, *Int. J. Mass Spec. Ion Proc.* **143,** 225 (1995).
47. A. Delcorte and B.J. Garrison, *J. Phys. Chem. B* **104,** 6785 (2000).
48. T.J. Colla, H.M. Urbassek, A. Wucher, C. Staudt, R. Heinrich, B.J. Garrison, C. Dandachi and G. Betz, *Nucl. Instrum. Methods Phys. Res. B* **143,** 284 (1998).
49. M.T. Robinson, *Phys. Rev. B* **40,** 10717 (1989).
50. J.F. Ziegler, J.P. Biersack and U. Littmark, in *The Stopping and Range of Ions in Matter*, Vol.1, Ed by Ziegler. Pergamon, New York (1985).
51. N. Winograd, in *Fundamental Processes in Sputtering of Atoms and Molecules (SPUT92),* Ed by P. Sigmund. Matematisk-fysiske Meddelelser, Copenhagen, p. 223 (1993).
52. A. Wucher and B.J. Garrison, *Phys. Rev. B* **46,** 4855 (1992).
53. B.J. Garrison, E.J. Dawnkaski, D. Srivastava and D.W. Brenner, *Science* **255,** 835 (1992).
54. A.M. Mueller and P. Chen, *J. Org. Chem.* **63,** 4581 (1998).
55. K.S. Feldman, R.F. Campbell, T.R. West, A.D. Aloise and D.M. Giampetro, *J. Org. Chem.* **64,** 7612 (1999).
56. E. Salonen, K. Nordlund, J. Tarus, T. Ahlgren, J. Keinonen and C.H. Wu, *Phys. Rev. B* **60,** 14005 (1999).
57. E. Salonen, K. Nordlund, J. Keinonen and C.H. Wu, *Europhys. Lett.* submitted.
58. H. Feil, J. Dieleman and B.J. Garrison, *J. Appl. Phys.* **74,** 1303 (1993).
59. See articles in *Radiat. Eff. Defects S.* **141–142** (1997).
60. See articles in *Nucl. Instrum. Methods B* **153** (1999).
61. The proceedings of the COSIRES meeting held in July 2000 at Penn State will be published in *Nucl. Instrum. Methods B*.
62. B.J. Garrison, A. Delcorte and K.D. Krantzman, *Accts. Chem. Res.* **33,** 69 (2000).
63. A. Delcorte, X. Vanden Eynde, P. Bertrand, J.C. Vickerman and B.J. Garrison, *J. Phys. Chem. B* **12,** 2673 (2000).

64. R.S. Taylor and B.J. Garrison, *Chem. Phys. Lett.* **230,** 495 (1994).
65. R.S. Taylor and B.J. Garrison, *Langmuir* **11,** 1220 (1995).
66. R.S. Taylor, C.L. Brummel, N. Winograd, B.J. Garrison and J.C. Vickerman, *Chem. Phys. Lett.* **233,** 575 (1995).
67. B.J. Garrison, *J. Am. Chem. Soc.* **104,** 6211 (1982); D.W. Moon, N. Winograd and B.J. Garrison, *Chem. Phys. Lett.* **114,** 237 (1985).
68. C.L. Brummel, I.N.W. Lee, Y. Zhou, S.J. Benkovic and N. Winograd, *Science* **264,** 399 (1994).
69. A. Delcorte and P. Bertrand, *Int. J. Mass Spectrom. Ion Processes* **184,** 217 (1999).
70. R.D. Harris, M.J. Van Stipdonk and E.A. Schweikert, *Int. J. Mass Spectrom. Ion Processes* **174,** 167 (1998).
71. R. Chatterjee, Z. Postawa, N. Winograd and B.J. Garrison, *J. Phys. Chem.* **103,** 151 (1999).
72. B.J. Garrison, *J. Am. Chem. Soc.* **102,** 6553 (1980); B.J. Garrison, *J. Am. Chem. Soc.* **104,** 6211 (1982).
73. M.M. Jakas and D.E. Harrison, Jr, *Phys. Rev. Lett.* **55,** 1782 (1985).
74. See, for example, C. Staudt, R. Heinrich and A. Wucher, *Nucl. Instrum. Methods B* **164,** 677 (2000).
75. P. Sigmund, *Phys. Rev.* **184,** 383 (1969).
76. P. Sigmund, in *Sputtering by Particle Bombardment I*, Ed by R. Behrisch. Springer, Berlin, p. 9 (1981).
77. P. Sigmund and C. Claussen, *J. Appl. Phys.* **52,** 990 (1981).
78. A. Miotello and R. Kelly, *Nucl. Instrum. Methods B* **122,** 458 (1997).
79. H.M. Urbassek, *Nucl. Instrum. Methods B* **122,** 427 (1997).
80. M.H. Shapiro and T.A. Tombrello, *Nucl. Instrum. Methods B* **152,** 221 (1999).
81. D.E. David, Th.F. Magnera, R. Tian, D. Stulik and J. Michl, *Nucl. Instrum. Methods B* **14,** 378 (1986); H.M. Urbassek and J. Michl, *Nucl. Instrum. Methods B* **22,** 480 (1987); G. Carter, *Radiat. Eff. Lett.* **43,** 193 (1979); G. Carter, *Nucl. Instrum. Methods.* **209/210,** 1 (1983); I.S. Bitenski and E.S. Parilis, *Nucl. Instrum. Methods B* **21,** 26 (1987); I.S. Bitenski, *Nucl. Instrum. Methods B* **83,** 110 (1993); J.F. Mahoney, J. Perel, T.D. Lee, P.A. Martino and P. Williams, *J. Am. Soc. Mass Spectrom.* **3,** 311 (1992); R.E. Johnson, B.U.R. Sundqvist, A. Hedin and D. Fenyo, *Phys. Rev. B* **40,** 49 (1998); Y. Kitazoe and Y. Yamamura, *Radiat. Eff. Lett.* **50,** 39 (1980); Y. Yamamura, *Nucl. Instrum. Methods* **194,** 515 (1982); R.P. Webb and D.E. Harrison Jr, *Appl. Phys. Lett.* **39,** 311 (1981); S.S. Wong and F.W. Rollgen, *Nucl. Instrum. Methods B* **14,** 436 (1986); B.U.R. Sundqvist, *Nucl. Instrum. Methods B* **48,** 517 (1990); K.T. Waldeer and H.M. Urbassek, *Nucl. Instrum. Methods B* **73,** 14 (1993).
82. L.V. Zhigilei and B.J. Garrison, *J. Appl. Phys.* **88,** 1281 (2000).
83. L.V. Zhigilei, P.B.S. Kodali and B.J. Garrison, *J. Phys. Chem. B* **101,** 2028 (1997); L.V. Zhigilei, P.B.S. Kodali and B.J. Garrison, *J. Phys. Chem. B* **102,** 2845 (1998).

84. G. Betz and W. Husinsky, in *Proceedings of the 12th International Conference on Secondary Ion Mass Spectrometry*, Ed by A. Benninghoven, P. Bertrand, H-N. Migeon and H. W. Werner. p. 13 (2000).
85. H. Kuhlewind, A. Kiermeier and H.J. Neusser, *J. Chem. Phys.* **85,** 4427 (1986).
86. S.J. Klippenstein, J.D. Faulk and R.C. Dunbar, *J. Chem. Phys.* **98,** 243 (1993).
87. Y. Gotkis, M. Oleinikova, M. Naor and C. Lifshitz. *J. Phys. Chem.* **97,** 12282 (1993).
88. M.W. Thompson, *Philos. Mag.* **18,** 377 (1968).
89. R. Chatterjee, D.E. Riederer, Z. Postawa and N. Winograd, *J. Phys. Chem. B* **102,** 4176 (1998).
90. M. Van Stipdonk, chapter in this volume.
91. G. Gillen, in *Proceedings of the 12th International Conference on Secondary Ion Mass Spectrometry,* Ed by A. Benninghoven, P. Bertrand, H-N. Migeon and H.W. Werner, p. 279 (2000).
92. See, for example, A.D. Applehans and J.E. Delmore, *Anal. Chem.* **61,** 1087 (1989); M.G. Blain, S. Della-Negra, H. Joret, Y. Le Beyec and E.A. Schweikert, *Phys. Rev. Lett.* **63,** 1625 (1989); J.F. Mahoney, J. Perel, S.A. Ruatta, P.A. Martine, S. Husain and T.D. Lee, *Rapid Commun. Mass Spectrom.* **5,** 441 (1991); F. Kotter and A. Benninghoven, *Appl. Surf. Sci.* **133,** 47 (1998).
93. J.A. Townes, A.K. White, E.N. Wiggins, K.D. Krantzman, B.J. Garrison and N. Winograd, *J. Phys. Chem. A* **103,** 4587 (1999).
94. T.C. Nguyen, D.W. Ward, J.A. Townes, A.K. White, K.D. Krantzman and B.J. Garrison, *J. Phys. Chem. B* **105,** 8221 (2000).
95. D.E. Harrison, Jr and C.B. Delaplain, *J. Appl. Phys.* **47,** 2252 (1976).
96. D.E. Harrison, Jr, P.W. Kelly, B.J. Garrison and N. Winograd, *Surf. Sci.* **76,** 311 (1978).
97. N. Winograd, B.J. Garrison and D.E. Harrison, Jr, *Phys. Rev. Lett.* **41,** 1120 (1978).

Author Questions

1) Scheme 1 is mentioned in the text and in the caption to Figure 7, but is not included.